Investigation of Metal Corrosion by In-Situ Electrochemical Force Microscopy

Thesis

Presented in Partial Fulfillment of the Requirements for Honors Research Distinction of the Degree Bachelor of Science from The Ohio State University

By

Corban Joyce

Undergraduate Program in Mechanical Engineering

The Ohio State University

2019

Thesis Committee

Dr. Hanna Cho, PhD, Advisor

Dr. Jung Hyun Kim, PhD

Abstract

Metal corrosion is a world-wide issue that affects millions of people and costs industries billions of dollars. In order to reduce the global impact of corrosion, new analyses must be conducted and new solutions must be created. In our current state, corrosion has been studied extensively at the macro level, but new technologies are emerging which permit the study of the corrosion process at much higher resolution – at a nanometer scale. This research project develops an in-situ characterization technique based on Atomic Force Microscopy (AFM) to take advantage of the ability to analyze the corrosion process at the nanoscale level in order to expand our knowledge of corrosion and suggest solutions to corrosion issues. With the researcher's background in the automotive industry and interest in the aerospace industry, the research is catered to these industries by focusing on particular alloys.

AFM and Kelvin Probe Force Microscopy (KPFM), which involve both topographic and electric potential imaging – are used to study the corrosion of metallic samples in various electrolytes. SKPM is used to obtain voltapotential information about a surface and Contact AFM is used to obtain topographical information. Scanning Electron Microscopy (SEM) and Energy-Dispersive X-Ray Spectroscopy (EdS) are also used to obtain information about the chemical composition of the sample surface.

As a result, the characterization technique developed in this research will help understand the onset of corrosion and its link to voltage potentials and chemical composition, ultimately providing suggestions to industry for improving the integrity of a vehicle's material composition. Topographical, electropotential, and chemical images embody the experimental results. Chemical images give insight to predict the initial nucleation of corrosion, whereas topographical and electropotential images characterize the corrosion process that occurs.

Conclusions regarding this research project are to be made with respect to the image results from AFM. Characterizations of the metal corrosion can be useful to automotive and aerospace companies for designing corrosion-resistant automobiles and aircraft. The ultimate goal of these conclusions is to suggest material selection, design, or composition to reduce corrosion.

Dedication

Dedicated to those who were helpful and patient with me as I pursued this academic endeavor.

Acknowledgments

I would like to acknowledge my advisor Dr. Hanna Cho for guiding me throughout the undergraduate research process. I would also like to acknowledge graduate students Sajith Dharmasena for teaching me the intricacies of Atomic Force Microscopy and Jian Liu for helping me accomplish my goals. Last but certainly not least, I would like to acknowledge Jun Wei Yap for helping me conduct many of my experiments, for without his efforts I would not be able to accomplish what is encompassed in this thesis.

I would also like to acknowledge the SVC REU funding, through a NSF IUCRC supported by NSF Grant IIP-1738723.

Vita

2015……...……..Kenston High School

2019…….B.S. Mechanical Engineering, Ohio State University

Fields of Study

Major Field: Mechanical Engineering

Table of Contents

List of Tables

List of Figures

Chapter 1. Introduction

1.1 Motivation

Metal corrosion is a world-wide issue that affects millions of people and costs industries billions of dollars. In fact, the global cost of corrosion in the single year of 2013 was over $2.5 trillion, equivalent to 3.4% of the global GDP [1]. Metal is ubiquitous in the modern world, and as the world becomes more dependent on metals, the risk of corrosion increases. In fact, large-scale industries have taken huge economic hits due to corrosion. In 2016, multi-national automaker, Toyota, agreed to pay $3.4 billion in settlements for a corrosion-related issue on its models [2]. It is evident that a gap exists in the field of knowledge related to corrosion.

In order to reduce the global impact of corrosion, new analyses must be conducted, and new solutions must be created. This may seem odd because most people know about or have heard of corrosion in some respect. They have learned about it in their chemistry classes, heard about it through some form of media, or maybe experienced it themselves in the common form of rust. From airplanes to automobiles, corrosion can exist anywhere an electrode and electrolyte are present. If so many people know of and understand corrosion, why is there an expensive gap in industry?

In our current state, corrosion has been studied extensively at the *macro* level [3], but new technologies have emerged which permit the study of the corrosion process at much higher resolution – at a *nanoscopic* scale. This research takes advantage of the ability to analyze the corrosion process at the nanoscale level in order to expand our knowledge of corrosion and suggest solutions to corrosion issues. In particular, we look at how it can be predicted and prevented by studying its relationship with voltage potential, topography, and elemental microstructure across the surface of a sample. Through the results of this study, the cost of corrosion can be curbed, and companies such as those in the automotive industry can focus their efforts on creating a product that is safer, more affordable, and of an overall higher quality.

With the researcher's background in and around the automotive and aerospace industries, the research is catered to these industries by focusing on particular alloys. With the automotive industry being such a large part of the economy and peoples' lives, an impact to the industry means an impact to millions of individuals across the globe.

1.2 Background

In order to combat corrosion, we must first understand its fundamental mechanism fully. Corrosion is a process in which metals degrade due the oxidation-reduction chemical reaction of particles on the metallic surface. There are many types of corrosion; however, they can be broken into two main groups for the purposes of this study: uniform and localized. From a practical standpoint, localized corrosion accounts for approximately 70

percent of material failures, and these failures are catalyzed by varying abnormalities affecting the metallic surface [4]. Fundamentally, corrosion requires the reaction of three main parts: metal, electrolyte, and oxygen. As depicted in Figure 1, water (electrolyte) makes contact with the surface of aluminum (metal), while in the presence of air (notably O_2). With these three parts in contact, the metal becomes polarized and electrons flow through the metal.

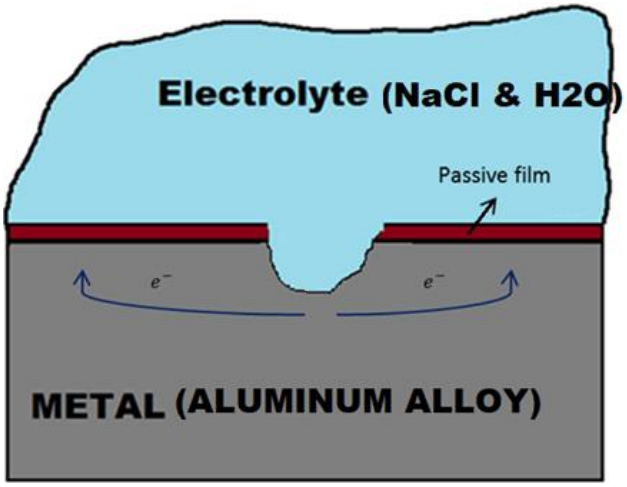

Figure 1: Electron Flow and Passive Film During Corrosion [ref]

While the overall corrosion mechanism is quite well understood, the corrosion process is specific to each material and affected by many factors like material defects and environmental factors (e.g., temperature, electrolyte type and concentration). In cases where there is corrosion in the common form of rust, there is ultimately a mass build-up of iron oxide. Although rust refers to corrosion of iron, corrosion can occur in many metals, and this research focuses on the corrosion of aluminum-based metal.

The alloy on which this research focuses is aluminum alloy 2024-T3. This alloy is quite common since it is used frequently in industry, and it exhibits corrosive behavior which this study seeks to replicate. Due to its composition, which will be described in Sample Preparation, it provides a balance of application to industry and ease of study. Elements other than aluminum are added to the metal to improve its performance for various applications. This generates an inhomogeneous distribution of microstructure on the alloy surface. Therefore, the susceptibility of aluminum alloys is drastically affected by its microstructure. This susceptibility can be seen practically and experimentally by the formation of galvanic cells at microstructured elements, as well as enhanced catalytic activity at the intermetallic boundaries.

1.3 Purpose

The purpose of this study is to build upon prior knowledge and overcome shortcomings of macroscale characterizations that can now be solved with new technology and methodology, specifically AFM-based techniques. Previous research has shown promise in predicting the onset of corrosion through its association with localized electric potentials. In addition, there has been industry and governmental demand for innovation in this area.

An example of previous AFM research on corrosion which compares electric potential and metallic topography over time can be seen in Figure 2 [5]. The AFM images shown in Figure 2 indicate a pattern between localized potential and future corrosion, i.e. high

potential concentration at 37 minutes, followed by corrosion pitting in the topography image at 144 minutes. This type of comparison between topography and potential is very similar to what this research study seeks to accomplish.

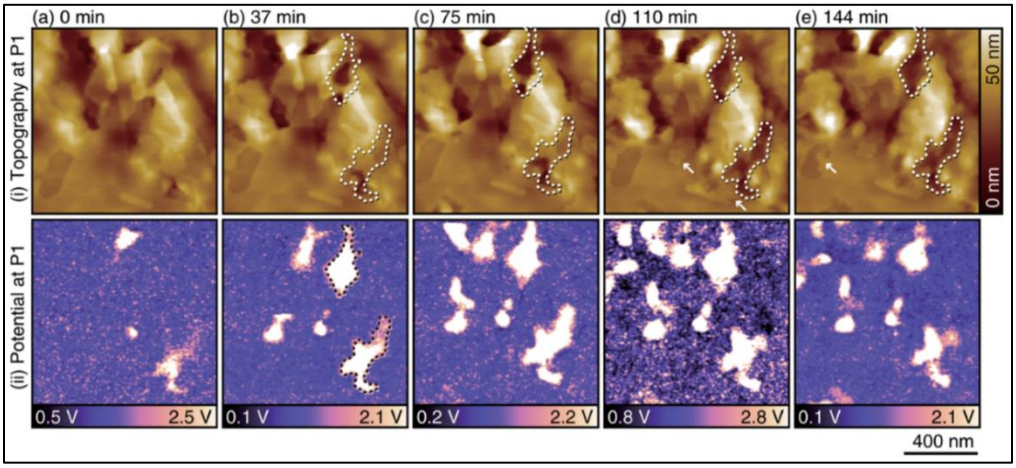

Figure 2: Topographic (top) and electric potential (bottom) images for duplex stainless-steel sample in a 10 mM aqueous solution [5]

While the previous study provides promising in-situ AFM data for stainless steel, this study aims to go beyond the previous study. In order to do so, it involves performing similar experiments but with a different kind of metal commonly found in vehicles, in environments that simulate real-world situations, i.e. aluminum alloy 2024-T3.

1.5 Objective

There are two parts to the original goals of this study. The first objective of this study is to complete the in-situ setup based on AFM which enables characterization of the local electrochemical process during corrosion with nanometer scale resolution. The setup will allow us to simulate and image the corrosion process over time under controlled

experimental settings, including electrolytes concentration and temperatures. The second objective of this study is to analyze corrosion and voltage potential images to understand the fundamental mechanism behind nucleation and propagation of corrosion. Previous studies have indicated that high localized electric potential can predict future corrosion. With the analysis of this pattern, this study can better characterize the nature of corrosion and further the research toward creating metal alloys or other solutions that are more resistant to corrosion.

Although not directly mentioned in the original scope of this study, the research naturally shifted to include yet another goal. The third research goal is to successfully image a single sample of the same area using EdS, SEM, SKPM, and AFM. The meaning and description of these method acronyms will be explained in the Methods section. Accomplishing this goal allows one to see three types of information about a single square area on the surface of a sample: chemical, electrical, and topographical. Connecting these pieces of information can bring light to the localized nucleation of corrosion.

Chapter 2. Methods

2.1 Microscopy Methods

The following methods are mentioned periodically throughout the report, and so this section serves to give the reader a basic understanding of each method and its use.

Atomic Force Microscopy (AFM) is the broadest form of force microscopy used in this research. It is used to obtain topographical information. This research only uses contact mode AFM and tapping mode AFM.

Electrochemical Force Microscopy (EFM) is a branch of Atomic Force Microscopy (AFM) which involves both topographic and electrochemical imaging. EFM serves as a broad term to describe the multiple forms of a force microscopy conducted throughout this research. While it has many uses, in this case, it is used to study the corrosion of metallic samples in an electrolyte.

SKPM is a form of EFM, primarily used in this research. SKPM is used to simultaneously obtain information about a surface related to its surface potential and its topography. Since surface potential is a driving factor in corrosion nucleation, SKPM is vital to achieving useful results. Because of how integral SKPM is to this research,

additional information will be provided on this method. In Figure 3 below, the dynamics of the cantilever during SKPM are shown. The diagram on the left of Figure 3 shows the two streams of information that are collect: topographic (1) and nap/potential (2). Due to the distance, ΔZ, between the cantilever and the surface, the potential difference between the cantilever and the surface can be measured. In our experimental setup, the surface is grounded, so the potential of the cantilever is the recorded potential seen on the image results.

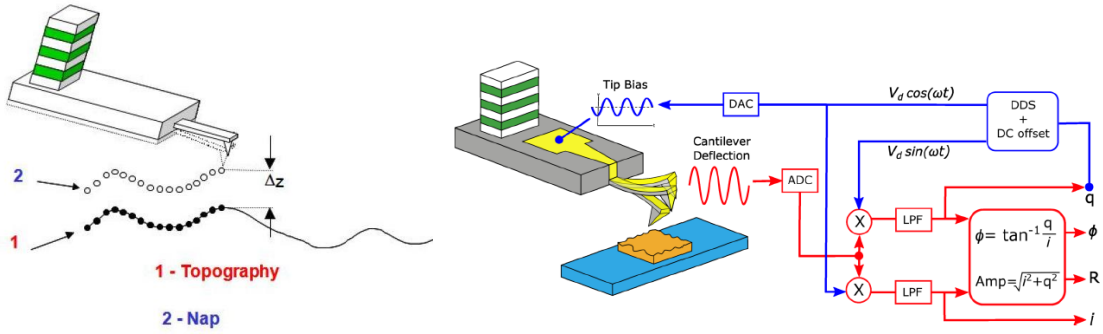

Figure 3: Diagram of SKPM cantilever (left), Controls/electronics of AFM (right)

On the right of Figure 3, the diagram focuses more on how the cantilever works, giving electrical and controls information. Though the innerworkings of the cantilever tip are not essential to understanding the results of this research, they are important for obtaining the best images during experiments. It is important, however, for the reader to understand that the yellow beam in Figure 3 is the "cantilever," and the pointed tip at the end is the "cantilever tip."

Examples of SKPM results collected in 2014 by Labukas and Strawhecker are shown in the following Figure 4 [6].

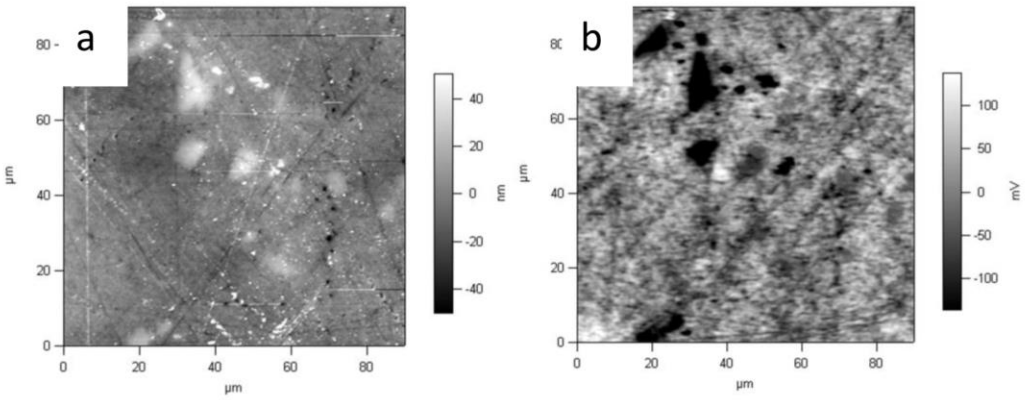

Figure 4: Example SKPM Images: (a) Topography, and (b) Voltapotential [6]

SEM is a different from the aforementioned forms of microscopy in that it does not involve directly touching the sample with a probe. Instead, it uses a beam of electrons. Essentially, it shoots electrons at a surface, depending on how they bounce back, it can determine what the surface looks like in a much faster fashion compared to AFM.

EdS is a unique form of imaging. It is similar to SEM in that it shoots a beam at the sample, except it uses measures energy levels as high-energy X-rays are emitted from the surface as the beam interacts with it. It is used to obtain information about the chemical composition of the sample surface, namely the elemental breakdown of the sample's microstructure. Based on the energy levels emitted from each point on the surface, it can determine the chemical composition at that point.

2.2 Experimental Methodology

Sample Preparation

The first step in the experimental process is sample preparation. The experimental process assumes that all devices and materials are readily available, were another researcher to attempt to replicate this study. Included in the assumed materials is sheet metal aluminum alloy 2024-T3. This metal alloy is the sample of primary focus in this research. The chemical composition of aluminum alloy (AA) 2024-T3 is shown in Table 1 [7]. The remainder of the composition (by weight) which is unaccounted for in the table is aluminum.

Table 1: Chemical Composition of Aluminum Alloy AA2024-T3 [7]

Element (Symbol)	Copper (Cu)	Magnesium (Mg)	Manganese (Mn)	Iron (Fe)	Silicon (Si)	Zinc (Zn)	Chromium (Cr)	Titanium (Ti)
% Comp.	3.8-4.9	1.2-1.8	0.3-0.9	0.5	0.5	0.25	0.1	0.05

This particular alloy was originally developed for structural components of aircraft, but it has become more ubiquitous since then. Due to its high strength-to-weight ratio, it has applications in gears, shafts, and fasteners. For anyone with experience in industry, it is apparent that these current applications require resistance to corrosion. More in-depth information about AA2024-T3 can be found in Appendix B.

In order to prepare the sample for analysis, a circle of 1 cm diameter must be cut from the sheet metal. To do this, a reciprocating saw was used to roughly cut the sample from the sheet. Afterward, the sample was grinded into a roughly circular cross-section. Now the sample is ready for polishing.

Each sample was polished at a polishing station in MacQuigg Lab at Ohio State University. The sample was first polished using the roughest grit, which was 240. The sample was lightly held against the polishing paper as the circular station turned at 120 rpm. Water was streaming across the grit throughout the polishing process for each of the paper grits. The sample was held in place for 30 seconds, turned 90 degrees to achieve polish in 2 directions, and held in place again for another 30 seconds. This process was repeated for each level of grit, which gradually increased from 240 to 400 to 600 to 800 to 1200.

After the sample achieved a polish equivalent to 1200 grit, the sample is further polished using diamond suspension. To do so, a polishing cloth is substituted in place of the grit paper on the table. Instead of water streaming over the surface, a diamond suspension is sprayed over the felt to wet the surface. The first diamond suspension contains 0.1-micron-sized diamond particles, which are used to achieve a finer polish that the grit paper. The same polishing process as the paper is conducted. This process is repeated again with 0.05-micron diamond suspension. The sample is carefully stored away to maintain the polish. After this, the polishing process is complete.

The penultimate step in preparing the sample is marking the surface. Using a fine, sharp cutting tool, the surface of the sample is scratched. This is done to serve as a landmark to be able to return to the sample and find the same area over and over. To remove potential scraps or burrs that may have accumulated on the surface during scratching, the surface is sonicated. The sonication process simply involves placing the sample in a bath of ethanol and sonicating for approximately five minutes. This process is repeated later in the experiment.

Scanning Electron Microscopy

The first microscopy method conducted on the sample is SEM. This form of microscopy is used to quickly image the sample and find areas of interest. The method is further described in the Microscopy Methods subsection.

The sample is placed into a SEM and the environment is vacuum-sealed. The images obtained from SEM are gray-scale, and do not contain the quantitative information essential to the significance of this research. Using SEM, a preliminary image of 500 micrometer scale is obtained. This image is used to find notable areas on the surface. Notable areas may be areas where there are many abnormalities in the surface. Surface abnormalities may signify areas of different chemical composition or abnormal microstructure. These are of particular interest because they are often ground zero for corrosion nucleation. An example of an SEM image is show in Figure 5.

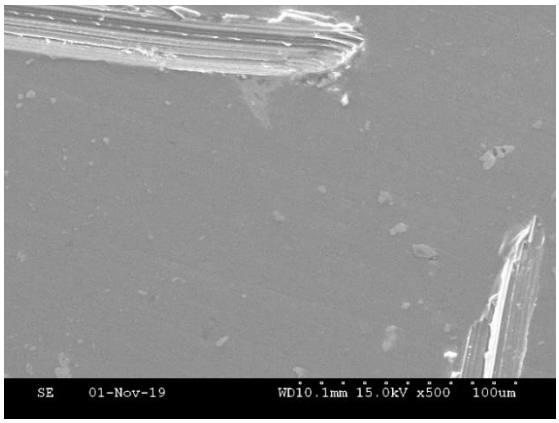

Figure 5: SEM Example Image

Once a notable area is found, additional SEM images are taken, ranging from 50-200 micrometer-scale, indicated at the bottom right of the SEM image. After this image is taken, the location of the notable area is documented, and the use of SEM is complete. EdS is the next imaging technology to be used.

Energy-dispersive X-ray Spectroscopy

The purpose of EdS in this scope is to obtain chemical information about the surface of the sample. It focuses on the same area of the sample that was notable using SEM. By shooting a beam of particles at the surface of the sample, this form of microscopy is able to obtain the sample's elemental information. Not only does it report the relative elemental breakdown of the sample area, but it also color-codes the local points across the surface, signifying various elements. An example result is shown in Figure 6. Blue represents aluminum, red represents copper, and green represents magnesium.

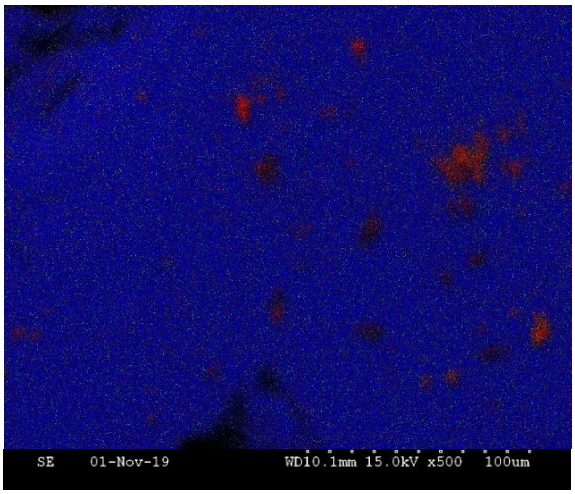

Figure 6: EdS Example Image

An EdS image is obtained of the same 100 micrometer-scale area found in SEM. Notable areas from EdS are those high in copper, signified by red areas. Since copper is highly electrically conductive, it is more likely to accelerate the onset of corrosion, making it more notable than other areas. These red areas will be focused on further in the following processes.

Sonication

Since the SEM and EdS are in different locations as the AFM, it is assumed that the surface of the sample becomes dirtied in the process of its transportation with the build-up of air particles. To prepare the sample for the remainder of the experiment, it must be cleaned thoroughly again. In order to clean the sample, it is placed in a sonic bath. The sample is submerged fully in ethanol and the sonication process is conducted for five

minutes. Afterward, the sample is removed and left to dry in air for 30 minutes. During the drying process, the setup for Scanning Kelvin Probe Microscopy (SKPM) begins.

Scanning Kelvin Probe Microscopy

Once the sample is dry, it is adhered to the center of the fluid cell using "Leitsilber" conductive silver paint. Before the paint dries, a copper wire is connected from the silver paint to ground. This grounds the sample so that the voltapotential of the sample may be measured. A picture of the setup described thus far can be found in Appendix A.

It should be noted that the experiment uses a liquid cell instead of an electrochemical (EC) cell. Early experiments did in fact use an EC cell, but due to the added versatility, ease, and simplicity of the fluid cell, the transition was made to use the fluid cell instead. All reported results are from experiments which used the fluid cell in the setup.

Next, the AFM software is started and put into contact AFM mode. In contact mode, no voltapotential information is collected yet. Contact mode AFM in this case is used analogously to SEM, in that it is used for preliminary images. Relatively large scans of 60x60 or 90x90 microns are conducted to locate the area of interest which was found originally in EdS images.

Once the desired area is located, the mode is switched to perform SKPM. A scan of the same 60x60 or 90x90 microns area is conducted. The size of the image depends on the

whether or not it captures enough notable areas. This scan contains information about the surface topography and surface potential. Areas of high or low surface potential are noted. Two or three areas of about 20x20 micrometers with surface potential local minima or maxima are chosen for the final stage of imaging. SKPM is then concluded and the next step is to add the electrolyte. This first step is shown using the diagram in Figure 7. The red line represents the laser being reflected off the back of the black cantilever.

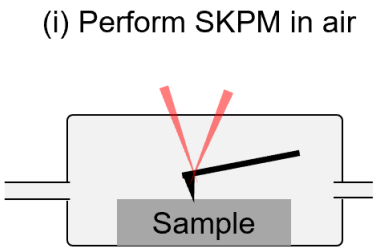

Figure 7: Step 1 in the SKPM/AFM imaging process

Electrolyte

The purpose of the electrolyte is to provide an electrical connection from one part of the surface to another. This models the common real-life scenario in which corrosion usually occurs. The electrolyte used is 0.1 M NaCl liquid electrolyte. In the real world, this electrolyte is very common due to the use of road salt on roads during the winter. Electrolyte is added to the fluid cell until it covers the surface of the sample. This is typically less than 10 mL. Figure 8 shows the second step in the SKPM/AFM imaging process, where the electrolyte is added to the fluid cell.

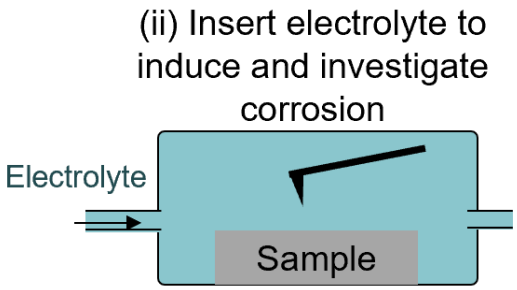

Figure 8: Step 2 in the SPKM/AFM imaging process

Atomic Force Microscopy (AFM)

SKPM cannot be conducted with the electrolyte because the electrolyte would short the electrical connection between the sample and the measurement tool – the cantilever tip. This electrical short would not only be dangerous and potentially harm the equipment, but it also would render any voltapotential information useless. Thus, Atomic Force Microscopy is used instead. AFM is used to obtain images related to surface topography only – not voltapotential.

In most results, contact mode AFM is used. Contact mode is the simplest form of AFM and it images the surface of the sample by dragging the cantilever tip across the surface and measuring the deflection of the cantilever.

As soon as the electrolyte is added to the fluid cell, AFM is conducted, as shown in Figure 9. Contact mode AFM is much quicker than SKPM, so scans of each of the notable areas can be conducted in a short period of time. Each scan is a square of 20-30

microns, depending on the area of interest's size; and it takes about 1 minute per scan. This scanning process is conducted on each of the noted areas with voltapotential local minima or maxima. After each area is scanned once, we wait 30 minutes from the first scan. Then, the scanning process is repeated again for each area. Using this process, two or three images are obtained every 30 minutes. This process is continued for 1.5 to 4 hours, depending on observed corrosive behavior and time availability.

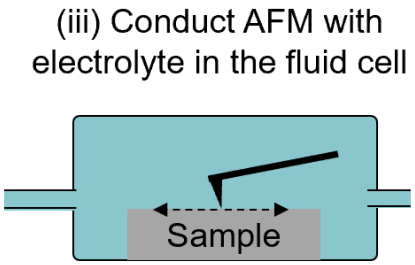

Figure 9: Step 3 in the SKPM/AFM imaging process (repeated)

Clean Up

After the experiment is finished, the electrolyte is properly disposed of and several other clean-up procedures are conducted. To remove the sample from the fluid cell, ethanol is administered into the cell. Ethanol breaks down the silver paint after a couple minutes and the sample can be removed using tweezers. The sample can be disposed of at this point since it is no longer needed. The same goes for the copper wire.

Post-Processing

Following the experiment, operations may be performed on the SKPM and AFM results to make them comparable and readable. Each SKPM and AFM image is modified using the "Flatten 1" modification within the Asylum Research software. Also, the image scales are standardized. Each image of the same type (height, deflection, zsensor, or potential) is given the same offset and range values. This permits easy comparison from one image to another.

In addition, areas of notable corrosive behavior are further analyzed to obtain specific quantitative height data along a particular line to characterize the morphological changes due to corrosion.

Chapter 3. Results

The results from this study will help understand the onset of corrosion and its link to voltage potentials and chemical composition. Topographical, electropotential, and chemical images embody the experimental results. Chemical images give insight to predict the initial nucleation of corrosion, and topographical and voltapotential images characterize the corrosion process that occurs.

Although many studies were conducted throughout the lifetime of this research project, this section will focus on the most useful results. With each experiment, the quality of results increases by refining procedure, images, and methodology. This fact is why the results are presented chronologically, so that the reader can understand the progression of the "investigation of metal corrosion."

Preliminary Results

As we developed the best procedure for collecting data, we periodically conducted experiments to gauge the success of our current progress. One of our early results which marked a significant breakthrough in capturing pitting corrosion is shown in the following figures. The material used as a sample in these results is AA6022-T4, which is a different, but similar, aluminum alloy than that which is used in the rest of the experimental results (AA2024-T3). AA6022-T4 was developed for automotive applications, with its high strength and corrosion resistance in mind. A preliminary

SKPM scan was taken and areas of local minima or maxima were noted in red and blue circles, as shown in Figure 10.

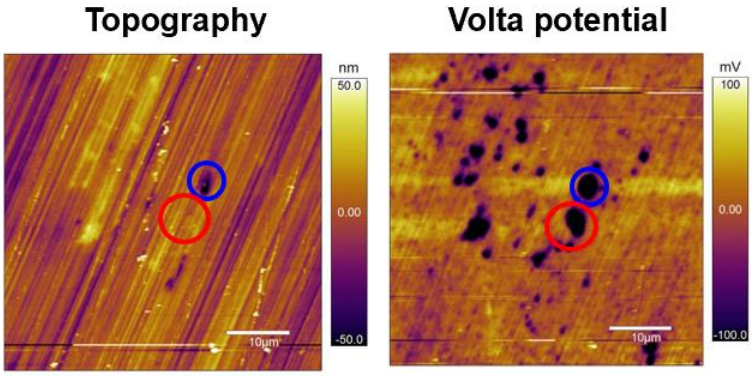

Figure 10: SKPM image results of: Topography (left), and Voltapotential (right)

Per Step 2 in the SKPM/AFM imaging process, electrolyte was added to the fluid cell and AFM was conducted. Two more topographical scans were captured, as shown below in Figure 11. These two scans were conducted 30 minutes apart and show the emergence of pitting corrosion in the red circle from the first scan to the next.

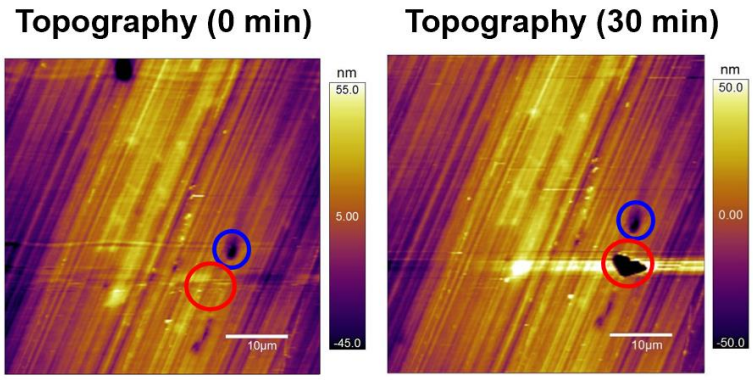

Figure 11: Time-dependent AFM images showing corrosive behavior

October 15, 2019 Results

As opposed to the previous experiment, this and the following experiments use a different aluminum alloy, AA2024-T3. The alloy primarily contains aluminum (90-95%), but it also consists of roughly 3-5% copper (by weight), 1-2% magnesium, and trace amounts of other metals such as manganese and iron. The specifics of the metal composition were defined in Table 1.

This experiment marks the beginning of implementing EdS and SEM fully into the data collection process. Images from these methods allowed sample areas of much higher quality to be studied, i.e. they gave hints at where corrosion will start. Although later SKPM scans were unable to show onset of corrosion, these images are important because they confirmed that it was possible to image the same area across three different machines, using three different methods: SEM, EdS, and SKPM.

The first set of images is from SEM. This is a relatively high-resolution image compared to other SEM images in this research, as it uses a 50-micrometer scale. In this scan, three notable areas are found and shown in the white circles in the figures. The left image is the original image and the right image is the same image rotated 93 degrees. The image is rotated to match the orientation of the sample of the SKPM/AFM images seen later in the experiment.

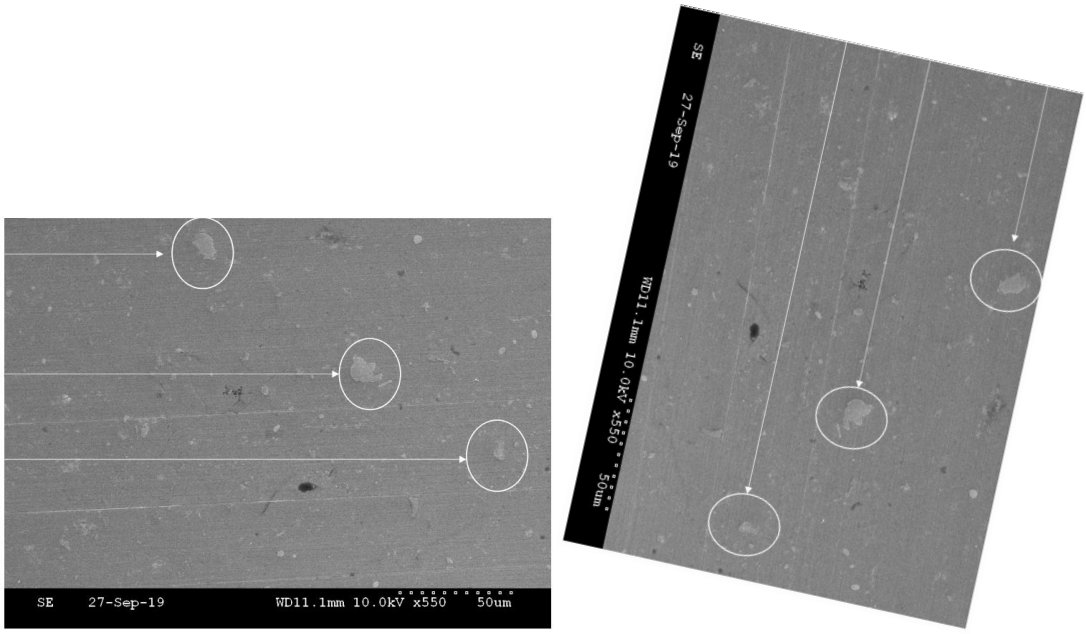

Figure 12: SEM Images: Unrotated (left) and Rotated (right)

After SEM, the next form of microscopy, EdS, was conducted. The EdS scan focuses on the same area as the SEM scan, and thus is done at the same scale (50 micrometer scale). Furthermore, the same notable areas are captured in square boxes, just as they were captured in circles in the SEM scan. The notable areas show up as clusters of red dots, where each dot corresponds to the element copper. It was this realization that allowed us to connect the surface abnormalities shown in SEM images to the concentrations of copper in the sample.

Also, the blue dots in the EdS image signify aluminum, and other colors correspond to minor concentrations such as magnesium, iron, silicon, and manganese. These chemical properties are show in Figure 13.

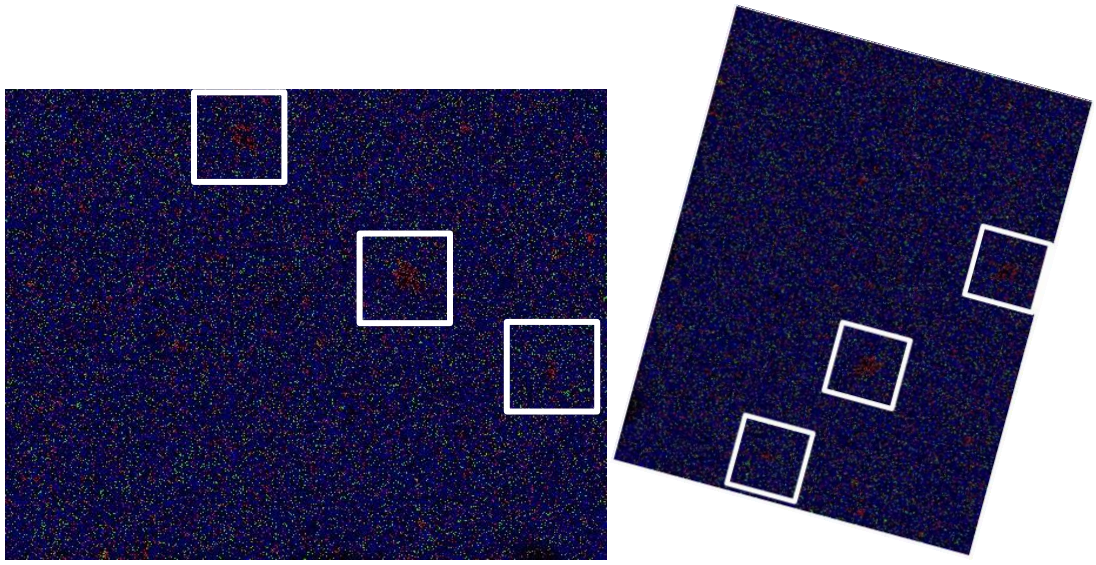

Figure 13: EdS Images: Unrotated (left) and Rotated (right)

After the notable areas had been found and characterized using SEM and EdS, the next step was to conduct SKPM. The blue square in Figure 14 captures the middle square in the unrotated picture in Figure 13. Since SKPM scans are much smaller than the previous scans, we focus on just one of the notable areas found in the SEM and EdS scans. These images marked the first instance of connecting SEM and EdS findings with SKPM results. This feat is difficult since SKPM/AFM is done on a different machine in a different location, and we were still experimenting with methods to best mark the surface to find the notable areas again after transport.

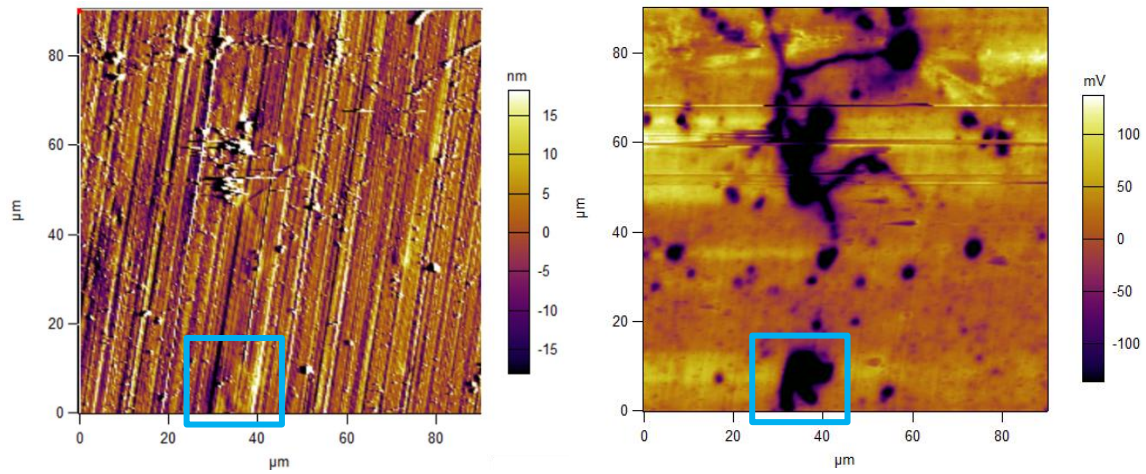

Figure 14: Initial SKPM Images: Amplitude (left) and Potential (right)

Corrosion testing was not conducted on this sample due to technical issues that arose during the AFM stage. However, the sample surface was thoroughly imaged, including the ZSensor scans shown in Figure 15. In the rightmost image in Figure 15, the ZSensor data focused on the notable area within the blue square is shown. This resolution of this image allows the user to see corrosion nucleation with the naked eye.

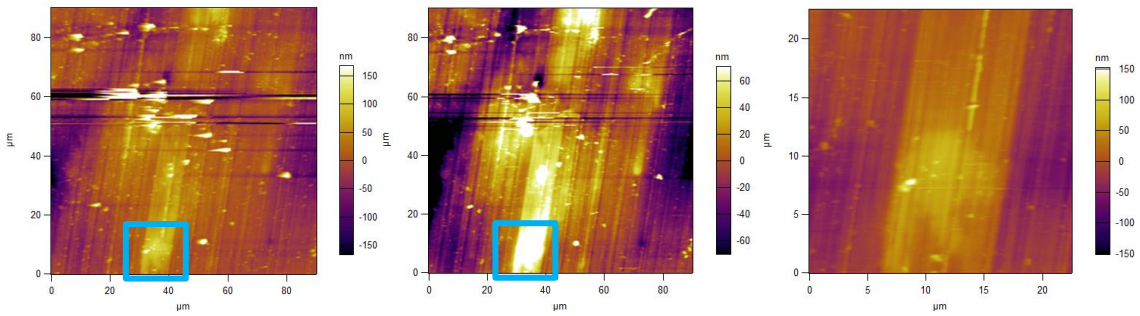

Figure 15: SKPM Image: ZSensor Scans (Initial, Scaled, Zoomed)

October 22, 2019 Results

The previous experiment had proven the possibility of connecting SEM/EdS scans to SKPM scans. This experiment took that knowledge and applied it in a much more thorough manner. The first image in Figure 16 shows the preliminary SEM scan that marks the beginning of each coming experiment. The image is at 100 micrometer resolution, which is large enough to find multiple areas of interest, yet fine enough to find details that denote potential areas of corrosion initiation. Two notable areas are captured in light blue boxes.

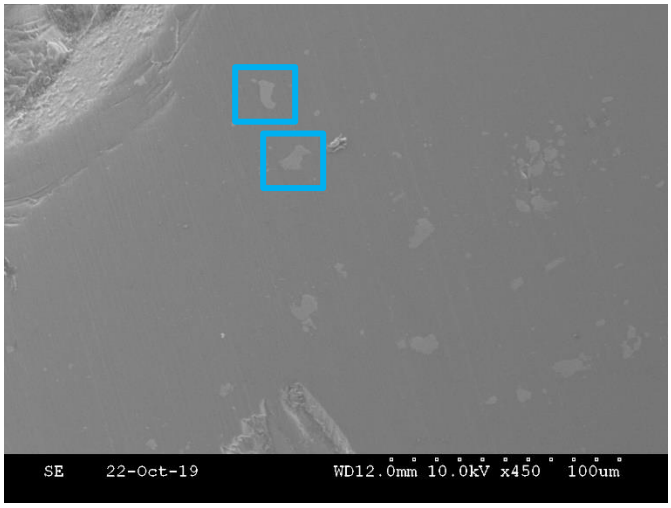

Figure 16: SEM Images: 100 Micrometer Scale Image

The second image shown in Figure 17 shows the histrogram-esque chemical breakdown obtained from the EdS scan. We will call this graph the EdS spectrum. The spikes in red correspond to the concentration of that element on the sample's sample. As the spectrum indicates, the three most prominent elements are aluminum (Al), copper (Cu), and magnesium (Mg). The third letter after the element symbol is either K or L. These

letters note the electron shell to which the emitted X-rays return; however, this information is not relevant to this research and can be ignored.

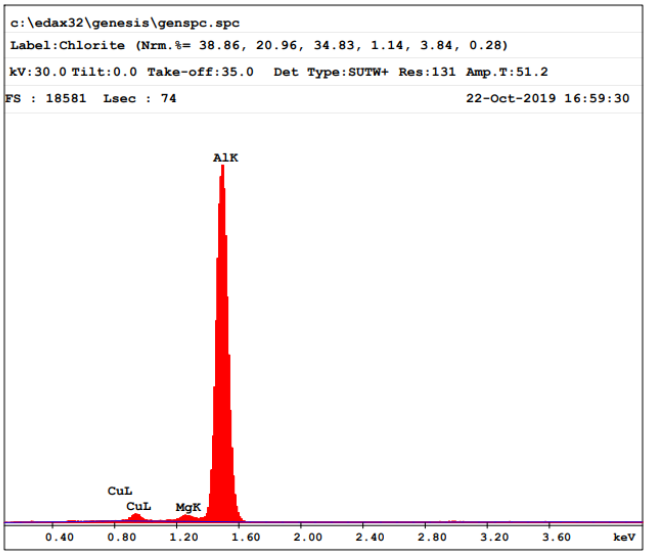

Figure 17: EdS Spectrum: Elemental Breakdown of Sample

The images corresponding to the EdS spectrum are shown in Figure 18. Again, the red areas correspond to copper and the blue areas correspond to aluminum. The light blue squares note the areas of interest which is further analyzed in the SKPM/AFM images.

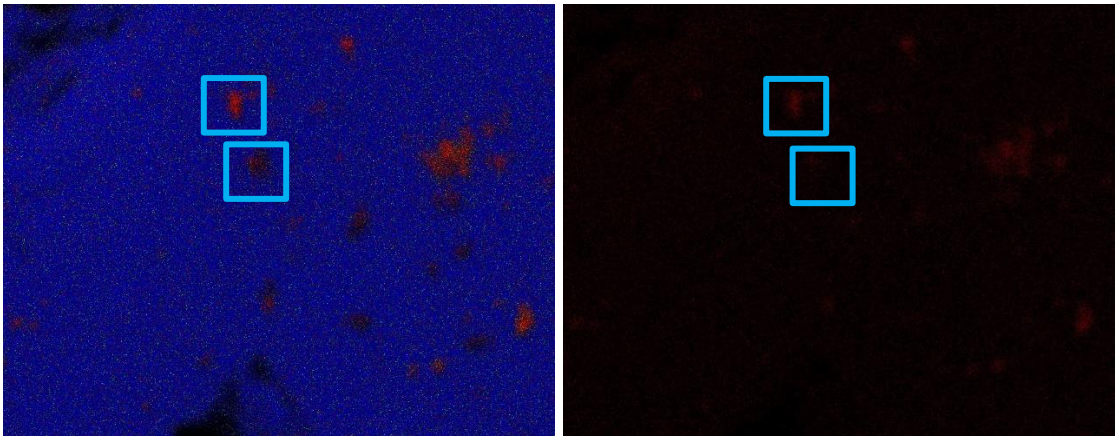

Figure 18: EdS Images: Overall Element Image (Al, Cu, Mg) (left), & Isolated Cu (right)

October 23, 2019 Results

The SKPM/AFM images were collected on the day following the SEM/EdS scans. An initial scan using contact mode in AFM was conducted to find the notable area shown in the SEM/EdS scans. After many unsuccessful scans, the notable area shown in Figure 19 is captured in the light blue squares.

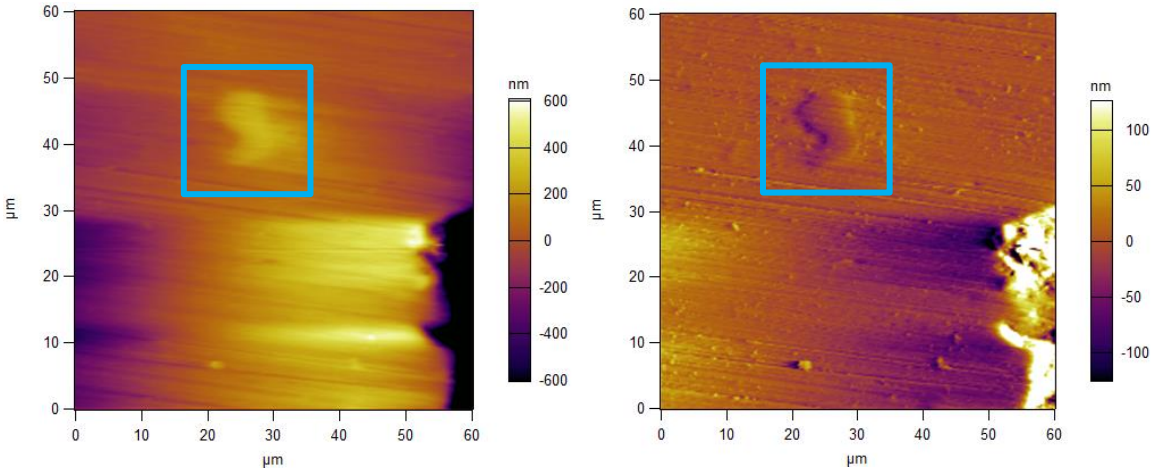

Figure 19: Contact AFM Image: Height (left) & Deflection (right) Initial Scan

The AFM was then switched to SKPM, and the following images were collected, as shown in Figure 20. After collecting this information, we were able to move forward with initiating corrosion.

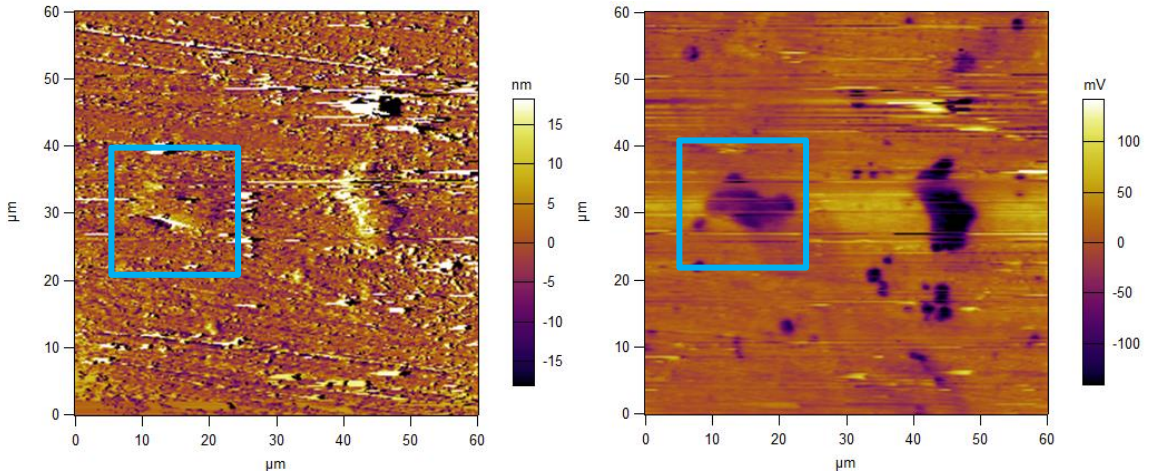

Figure 20: SKPM Image: Amplitude (left) & Potential (right) Initial Scan

The results in Figure 21 show the time-dependent Deflection and ZSensor information about the notable area found in Figure 20. The first scan was conducted shortly after the electrolyte was added to the liquid cell, and each subsequent image was conducted 30 minutes after the previous.

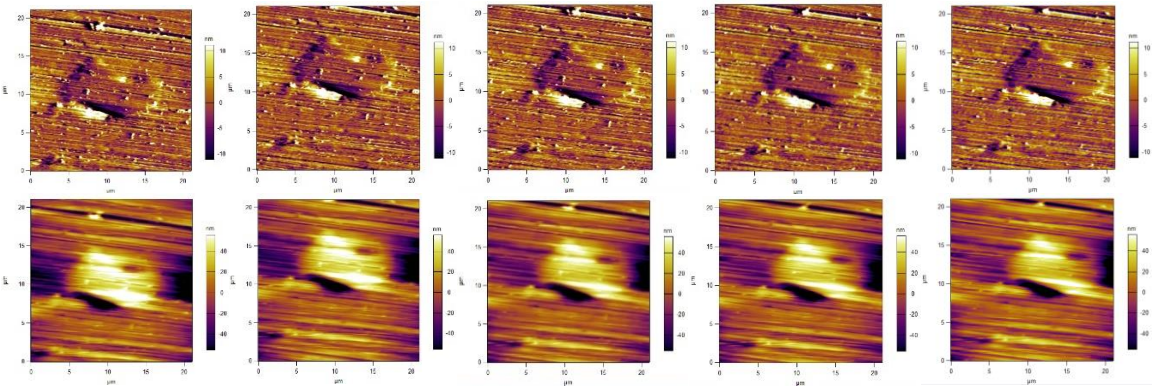

Contact AFM Image: Deflection (top) & ZSensor (bottom)

Unfortunately, no significant corrosive behavior was observed across the periodically collected scans. Minor changes in particles on the surface can be observed, but the pitting corrosion which we would have liked to observe did not occur. However, this

experiment proved that our experimental setup permitted these types of images to be collected over time.

November 1, 2019 Results

The following results mark the final and most extensive, thorough analysis of the sample at hand. Like the previous experiments, analysis of the sample starts with SEM imaging, followed by EdS imaging. In Figure 21, the left image shows two scratches in the surface at a large scale; one scratch is roughly horizontal, while the other scratch is roughly vertical. The right image gets a closer look at the surface by increasing the resolution from 200 micrometer-scale to 100 micrometer-scale. These scratches serve as markers to find the same notable areas again when conducting SKPM/AFM. This method of marking the surface was adopted because the previous method of using a Sharpie marker became futile. During sonication of the sample, the Sharpie marker dissolved. However, the scratching technique allowed for a more permanent sort of mark.

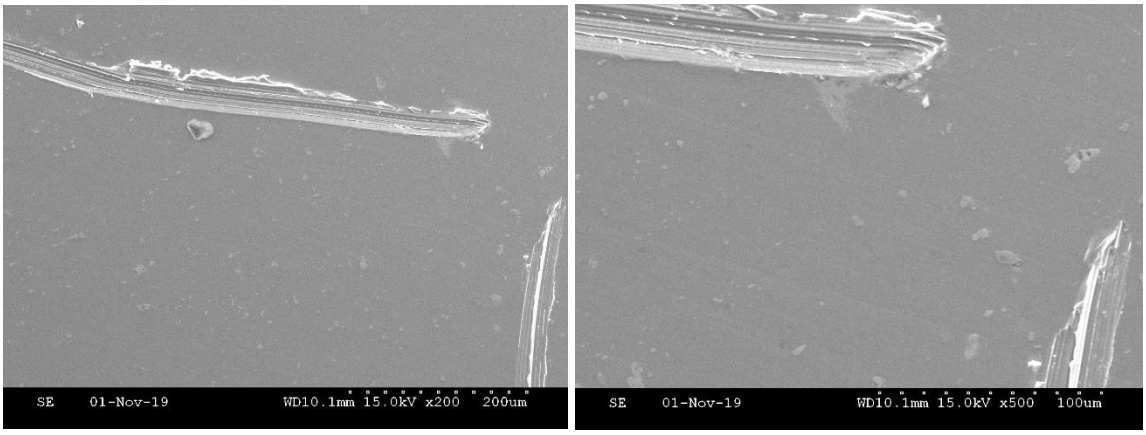

Figure 21: SEM Images: 200 Micrometer Scale (left) & 100 Micrometer Scale (right)

The scratches are still visible in the EdS images, as shown in Figure 22. Once again, the blue dots correspond to aluminum, and the red dots correspond to copper. Three notable areas of high copper concentration are captured in the squares in Figure 22. To further note the copper concentration, all elements beside copper were removed from the image on the right.

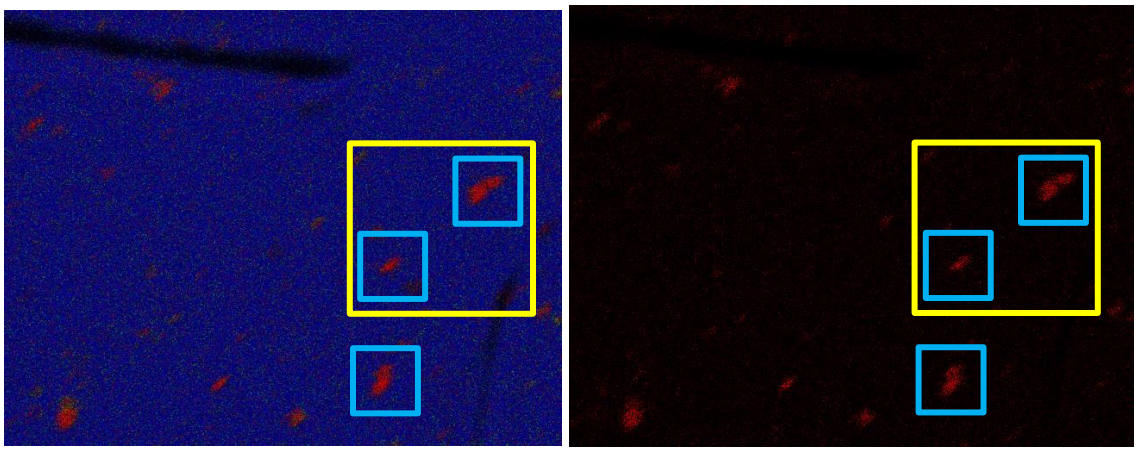

Figure 22: EdS Images: Overall Element Image (Al, Cu, Mg) (left), & Isolated Cu (right)

The large yellow squares signify the area which is pursued further in the following AFM images.

November 2, 2019 Results

The preliminary AFM images are shown in Figure 23. In the bottom right corner of both images is the edge of the vertical scratch shown earlier in the SEM and EdS images. This scratch serves as a reference and is perceived as a bright area in the AFM images. Figure 23 and Figure 24 focus on the yellow square shown in Figure 22, with a focus on the two notable areas within that yellow square.

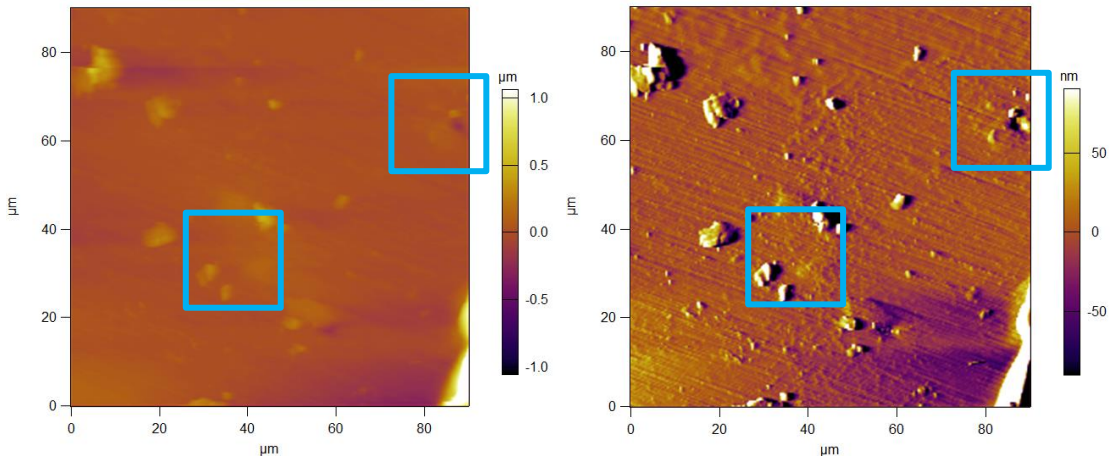

Figure 23: Contact AFM Image: Height (left) & Deflection (right)

In Figure 23 and Figure 24, the notable areas are captured by light blue squares. Interestingly, the areas which had high concentrations of copper as seen in the EdS images, do not have significantly high height and deflection values. However, the presence of the copper becomes apparent in the image on the right of Figure 24. There are dark areas representing areas of low surface potential in each square.

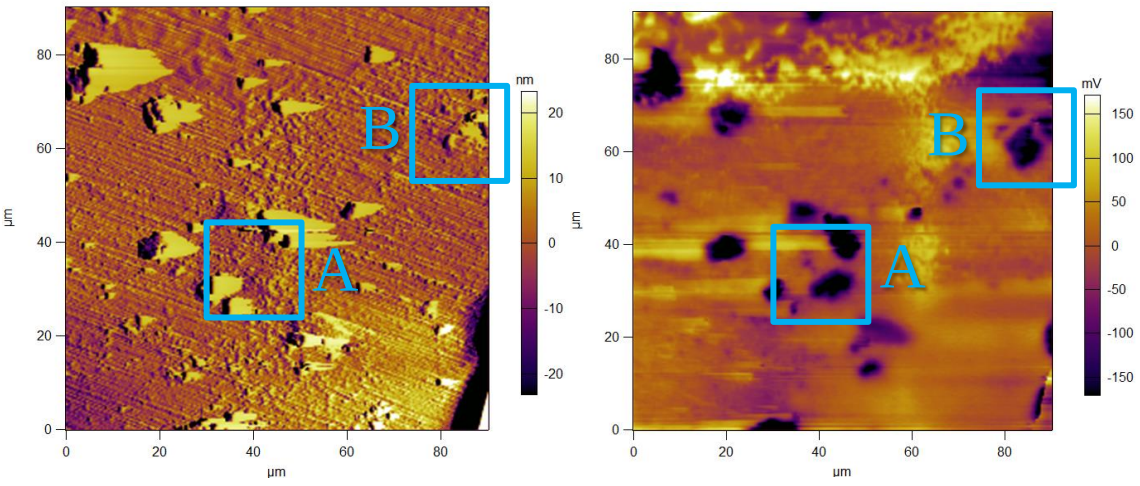

Figure 24: SKPM Image: Amplitude (left) & Voltapotential (right), t = 0 min

To maximize the probability of capturing the occurrence of corrosion, both of the aforementioned areas were imaged over time using AFM. The bottom left square is called Location A, and the upper right square is called Location B. The progression of Location A after the electrolyte was added is shown in Figure 25. The time, t = 0 min, refers to the amount of time after the electrolyte was added to the fluid cell.

There is no significant corrosive behavior observed at Location A. Particles become more prominent, especially in the image of Deflection at t = 60 min. However, this may be due to the arbitrary quality of the scan. Therefore, we cannot attribute those changes to corrosion.

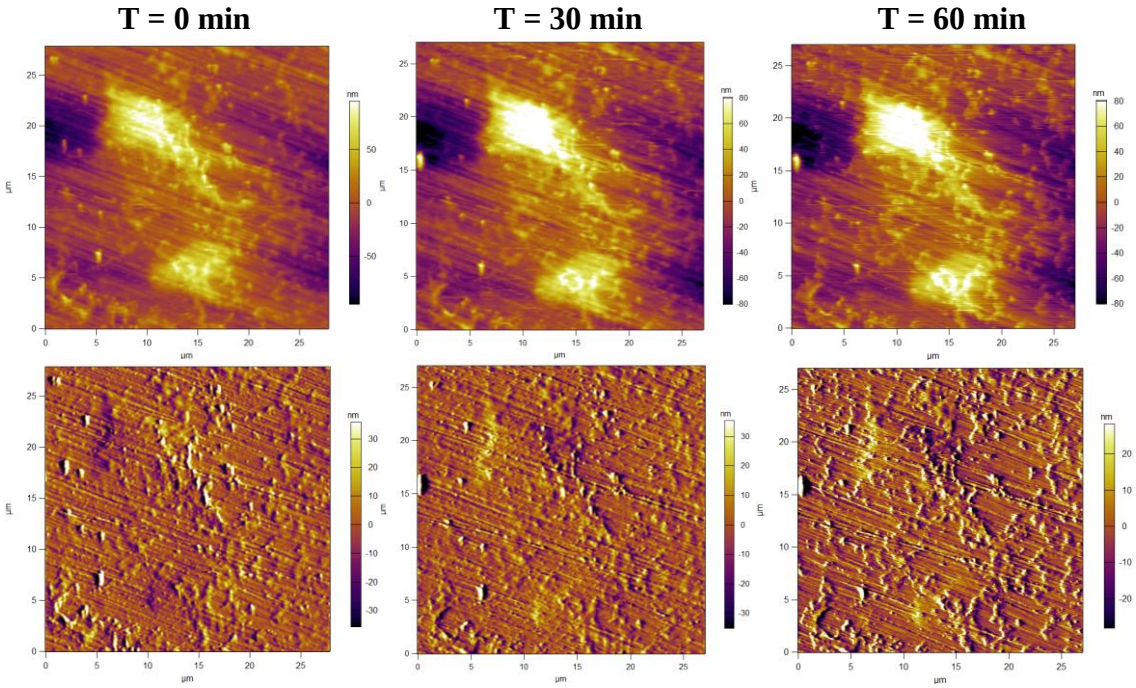

Figure 25: Contact AFM: Height (top) & Deflection (bottom), Location A

The progression of Location B after adding the electrolyte is shown in Figure 26. More significant changes occurred in Location B, which can be attributed to corrosion. The

area of significant corrosive behavior is captured in the light blue square. From t = 30 to t = 60, it is clear that a change occurs, as highlighted by the yellow circles.

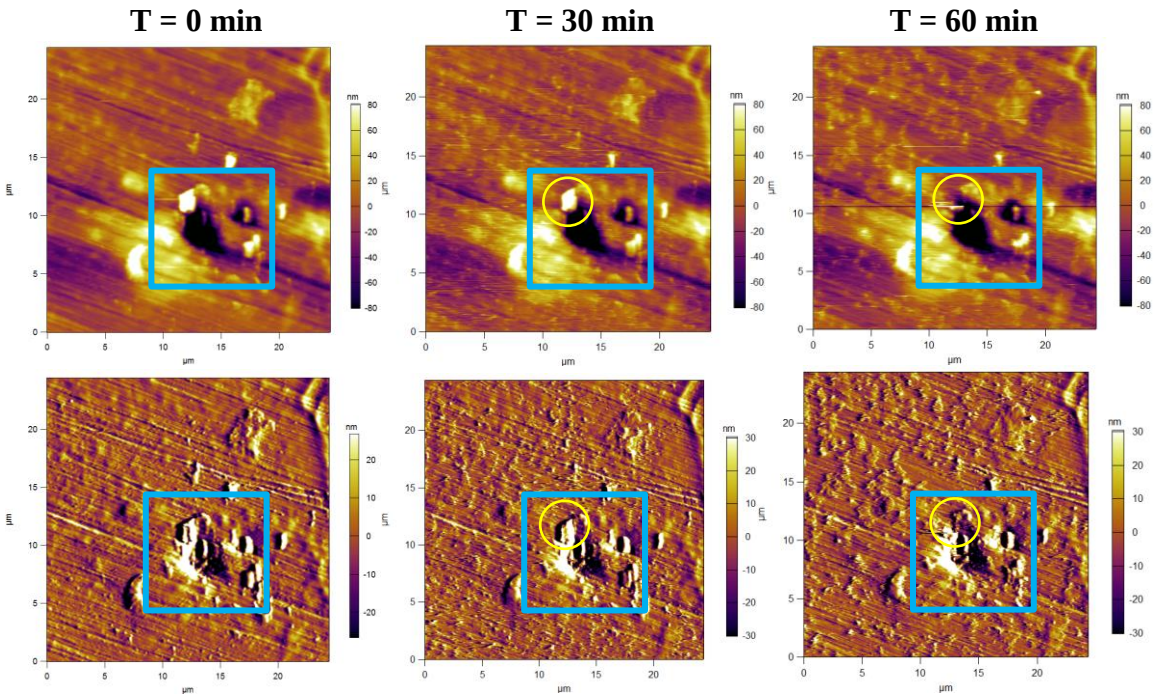

Figure 26: Contact AFM: Height (top) & Deflection (bottom), Location B

However, the change shown within the yellow circles may be due to interference by the AFM cantilever tip, so we will also look at other aspects of the surface. To get a more precise idea of the progression of corrosion, we analyze a single line across the surface, as indicated in Figure 27. The line of interest is a horizontal line at Y = 8.50 ± 1 micrometer.

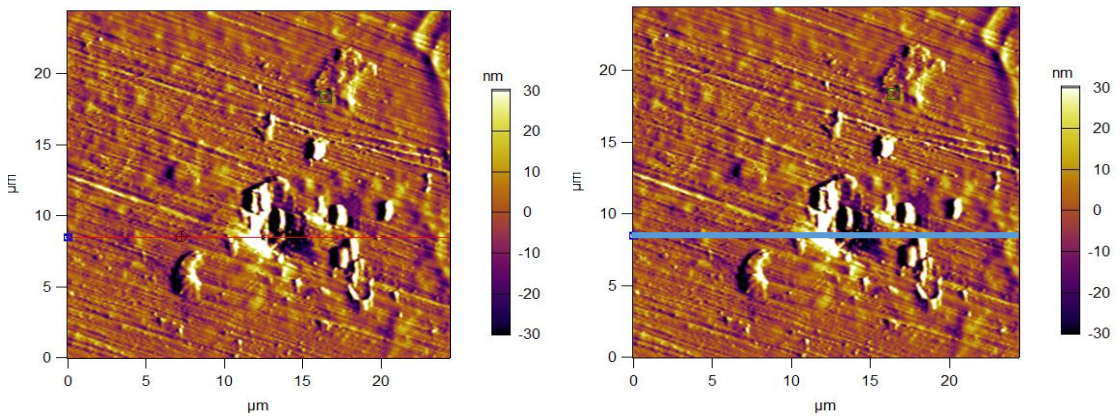

Figure 27: Contact AFM Image: Line of Interest (left), & Bolded Line (right), Location B

The cross-sectional profile of the surface at this line is shown in Figure 28. The profile changes over time, so the profile is collected at each time increment: t = 0, 30 and 60 minutes. The three profiles are laid over each other to directly compare them. There are a couple important observations that can be made as a result of this comparison. Firstly, the low point, AKA the pit, becomes deeper over time. Grooves become sharper as time progresses, indicating that mass has moved out of the pit. Secondly, mass build-ups have accumulated outside of the pit, indicated by arrows. With the mass leaving the pit and accumulating around it, we can infer that this mass transfer has occurred.

According to the rough approximations which can be drawn from the voltapotential image in the SKPM scan in Figure 24, the mass transferred from an area of initial low voltapotential to areas of higher potential. This mass transfer matches the corrosive behavior which we predicted. Electrons flow from anode (low voltapotential) to the cathode (high voltapotential), and over time, significant mass was transferred.

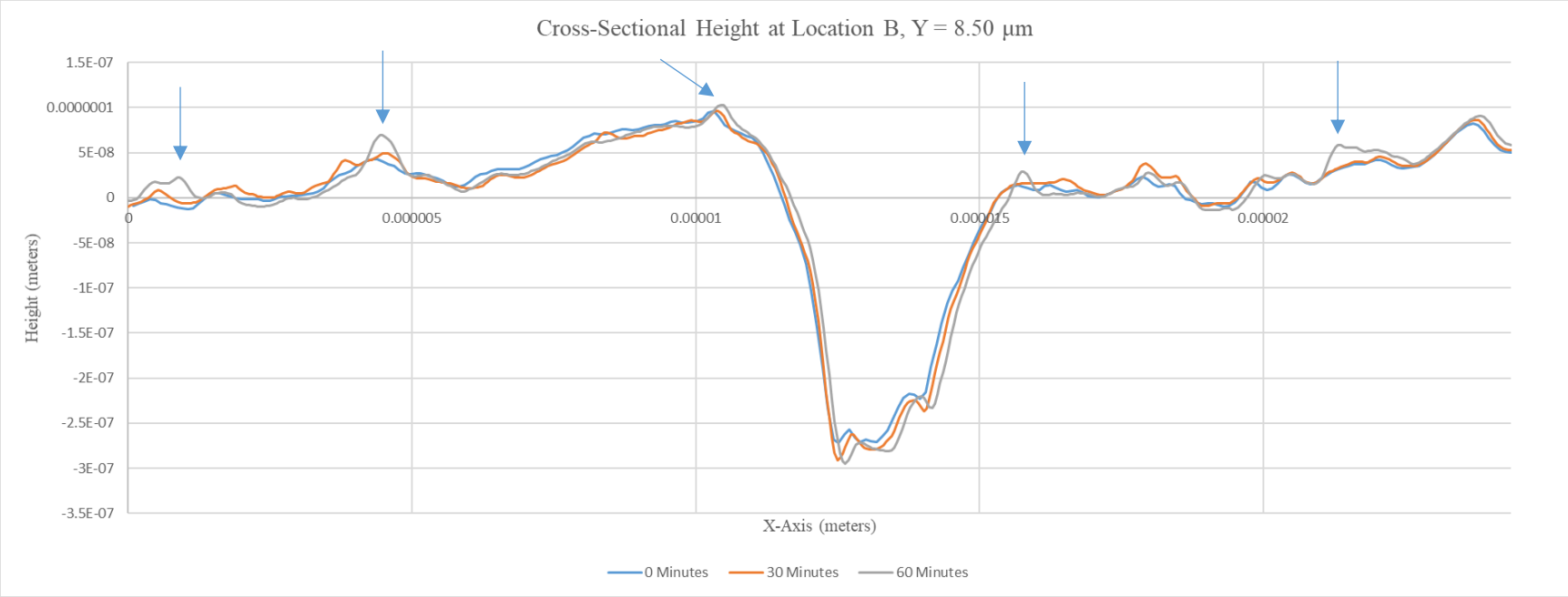

Figure 28: Cross-Sectional Height at Location B, Y = 8.50 µm

Chapter 4. Conclusion

Conclusion

Conclusions regarding this research project are to be made with respect to the image results from Electrochemical Force Microscopy. Characterizations of the metal corrosion can be useful to automotive and aerospace companies for designing corrosion-resistant automobiles and aircraft. The results of this research contain data that is useful to industry and to the field of corrosion overall.

The three research goals described at the beginning of this report were completed. The first research goal was to complete the in-situ Electrochemical-AFM (EC-AFM or EFM) setup which enables characterization of the local electrochemical process during corrosion with nanometer scale resolution. Accomplishing this goal served as the first step toward completing the greater goals of the research. The experimental setup was defined and described throughout the report.

The second research goal was to analyze topographical and voltapotential images to understand the fundamental mechanism behind nucleation and propagation of corrosion. Topographical and voltapotential images were captured and shared in this report by means of the methods SKPM and AFM. These images supported our hypothesis which

asserted that there is a connection between surface topography and voltapotential across a metallic surface. This hypothesis also includes the assertion that voltapotential extremities serve as the corrosion nucleation areas. In the final section of the results, this connection about the electrical nature of corrosion is made.

In addition to making the connection between corrosive behavior and voltapotential extremities, this research also connected the voltapotential to the chemical composition of the sample. That is, areas of high voltapotential often also corresponded to areas where the metal had been alloyed. For example, areas where copper had become clustered on the primarily aluminum surface tended to exhibit high voltapotential. This observation makes sense in light of the electrical properties of copper, namely that it is highly electrically conductive. These observations satisfied the third research goal by connecting the local chemical composition of the sample to its surface topography and voltapotential.

Future Work

With every consecutive experiment during this research study, it was obvious that there were ways to improve. Each experiment improved upon the last. However, the experiments had to come to an end. Therefore, the final experiment gave rise to many ideas for ways to improve the next experiment, as well as new experimental methods to investigate. So that these ideas are not lost, they will be transcribed in this section.

In order to improve the quality of images while the sample is submerged in electrolyte, we suggest using the tapping mode, instead of contact mode of AFM. It is also known as AC mode. This method is more complicated than contact mode, but it has the potential to provide better quality images. The logic behind this suggestion is twofold. First, tapping mode is less likely to interfere with the surface by dragging or moving particles. Secondly, empirically, data collected in tapping mode tends to be of higher resolution than data collected in contact mode, especially in cases where the surface is sensitive to touch. In effect, the images received from tapping mode provide a higher likelihood of capturing subtle changes in surface topography.

In addition to the changes that can be made to the methodology of this research, there are many nuances upon which one can improve. Many aspects of the experimental procedure were based on general practices, intuition, or suggestions from experts. However, research is a venture into uncharted territory, so not much can be certain. Small optimizations can be made to not only improve the quality of results, but also make the experimental procedure more efficient. Experimental parameters can be optimized, such as the time that the sample spends in the sonic bath, the time between each AFM image capture, the size of each image scan, and more.

Bibliography

[1] Jacobson, Gretchen. "Economic Impact: Assessment of the Global Cost of Corrosion." *NACE Impact*. http://impact.nace.org/economic-impact.aspx.

[2] Randazzo, Sara. "Toyota in $3.4 Billion Settlement Over Corrosion in Some Trucks and SUVs." *The Wall Street Journal*. https://www.wsj.com/articles/toyota-in-3-4-billion-settlement-over-corrosion-in-some-trucks-and-suvs-1478972740.

[3] Schmutz, P. and Frankel, G.S. "Corrosion Study of AA2024-T3 by Scanning Kelvin Probe Force Microscopy and In Situ Atomic Force Microscopy Scratching." *Journal of The Electrochemical Society*, vol. 145, no. 7, July 1998, pp. 2295.

[4] Nimmo, Bill and Hinds, Gareth. "Beginners Guide to Corrosion." *NPL*. http://resource.npl.co.uk/docs/science_technology/materials/life_management_of_materials/publications/online_guides/pdf/beginners_guide_to_corrosion.pdf.

[5] Honbo, K., Ogata, S., Kitagawa, T., Okamoto, T., Kobayashi, N., Sugimoto, I., Shima, S., Fukunaga, A., Takatoh, C., and Fukuma, T., "Visualizing Nanoscale Distribution of Corrosion Cells by Open-Loop Electric Potential Microscopy." *ACS Nano*, vol. 10, no. 2, 2016, pp. 2575-2583.

[6] Labukas, Joseph P. and Strawhecker, Kenneth E., "Scanning Probe Investigation of Pitting Corrosion on Aluminum 5083 H131." Army Research Laboratory. May 2014, pp. 6. https://pdfs.semanticscholar.org/5243/537ec6e284bde69e72387b6b98e32924cb7e.pdf.

[7] Guillaumin, V., Schmutz, P. and Frankel, G. S., "Characterization of Corrosion Internfaces by the Scanning Kelvin Probe Microscopy Technique." *Journal of The Electrochemical Society*, vol. 148, no. 5, B165, 2001, pp. 163-173.

[8] "High-Strength 2024 Aluminum Sheets and Bars." *McMaster Carr*. https://www.mcmaster.com/catalog%2f125%2f3818

Appendix A. Additional Figures

Figure A 1: AFM Head being placed on main stage

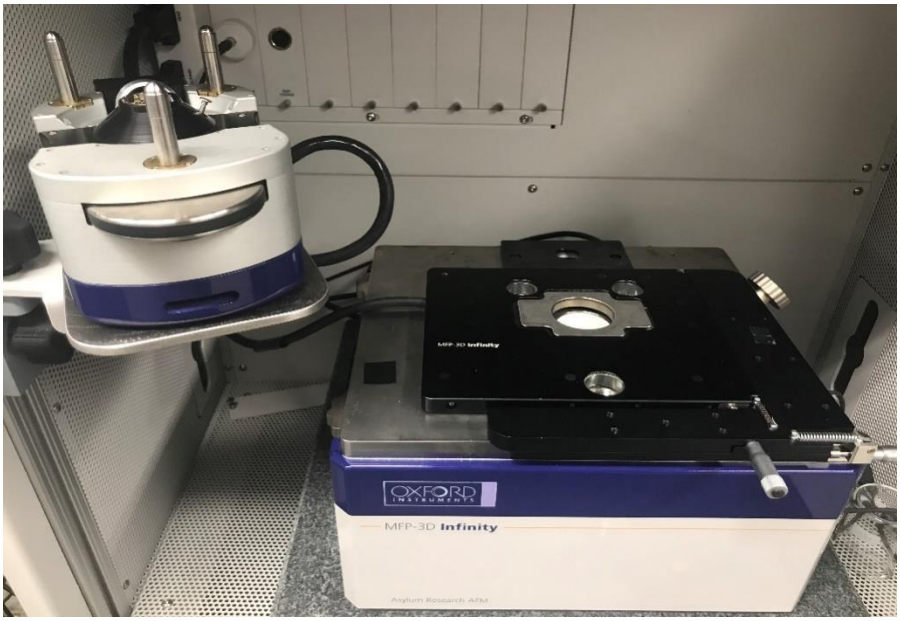

Figure A 2: Atomic Force Microscope Setup (head on left, stage on right)

Figure A 3: 3D Standard Cantilever Holder in Black Mount

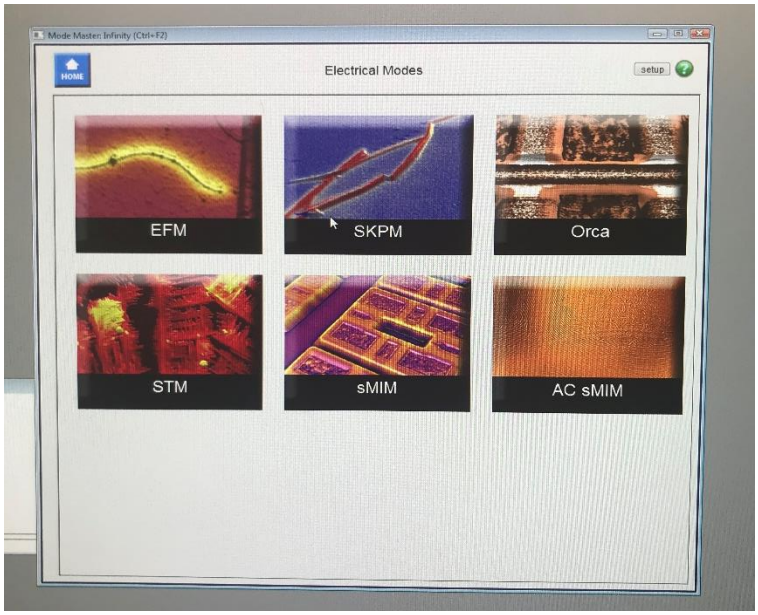

Figure A 4: Electrical Modes in Asylum Research Software (SKPM in top middle)

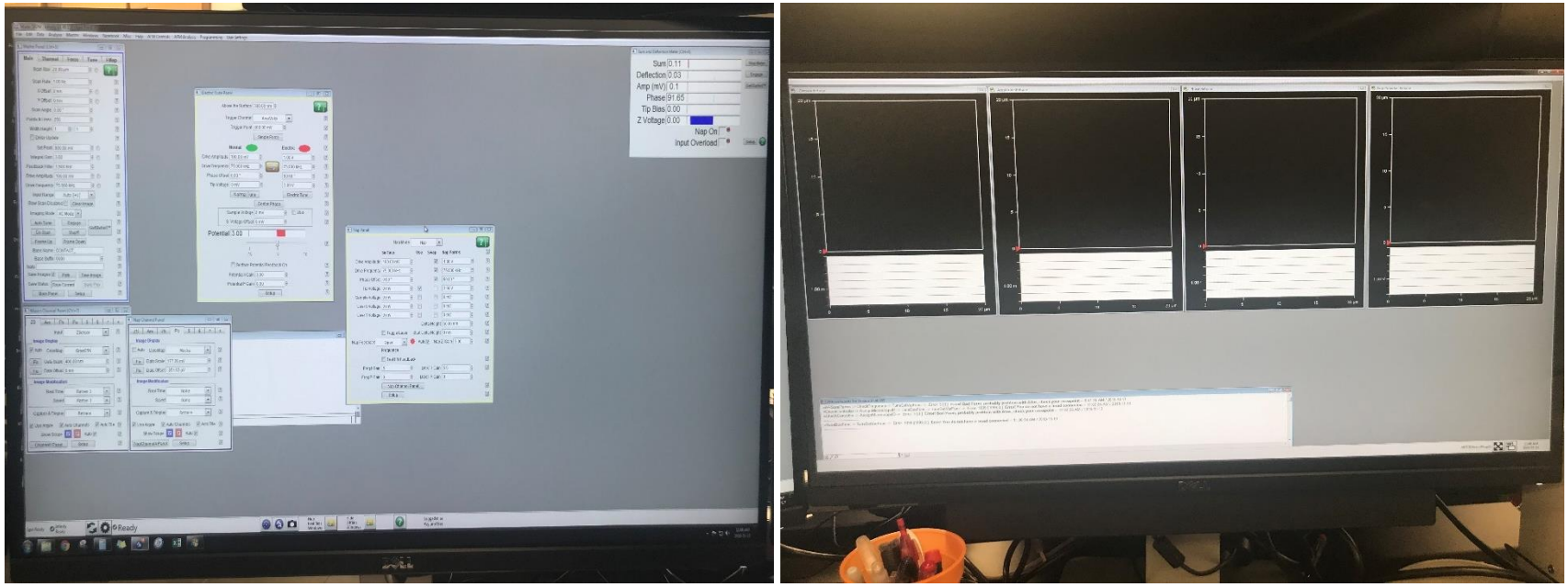

Figure A 5: Dual Monitor Setup with Configuration (left) and Real-Time Images (right)

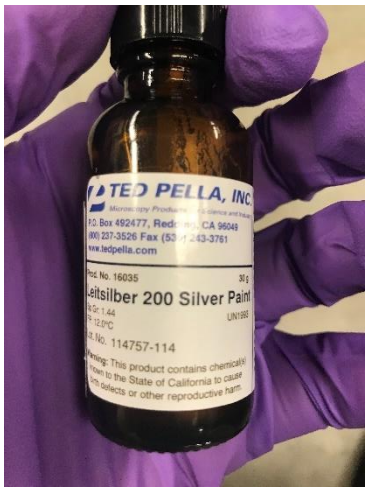

Figure A 6: Leitsilber 200 Silver Paint conductive adhesive

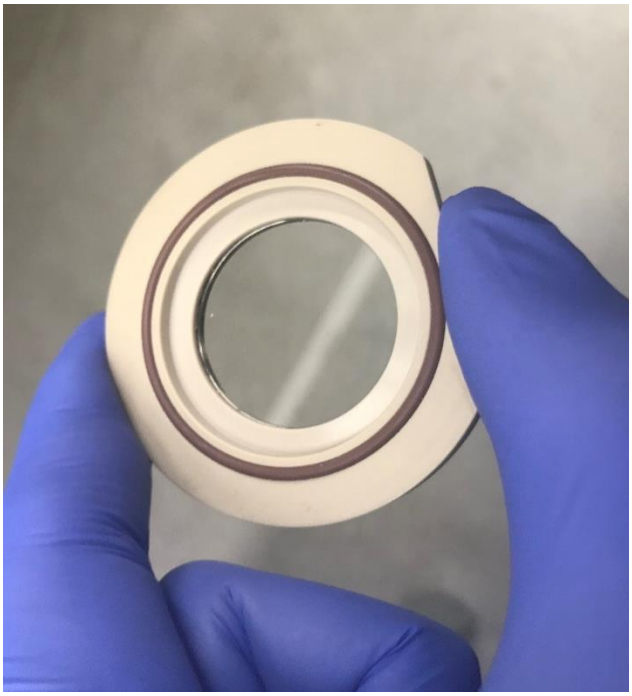

Figure A 7: Fluid Cell

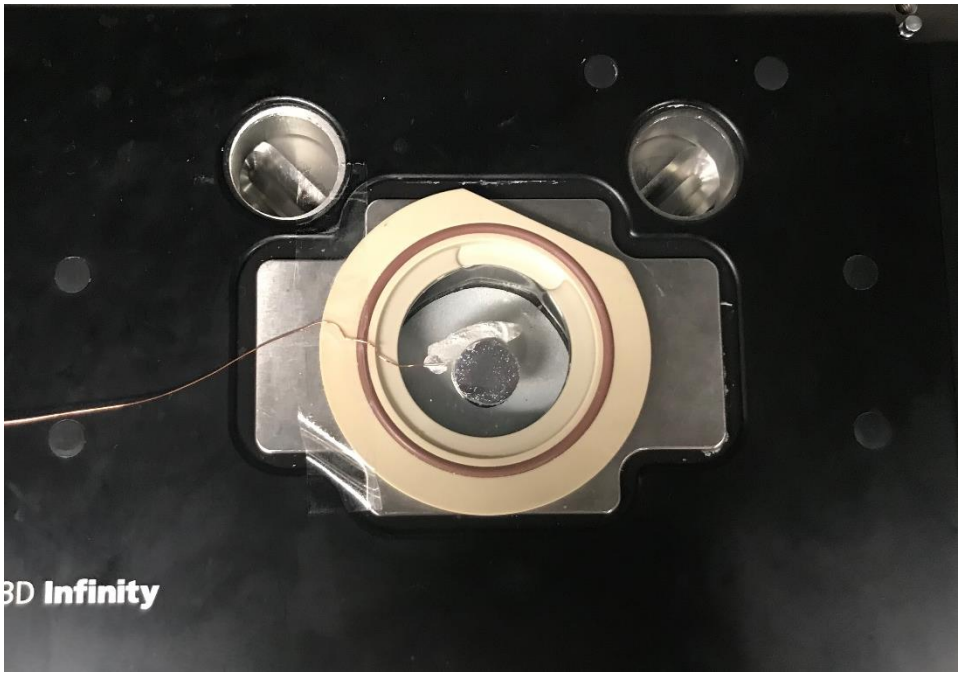

Figure A 8: Top View of Liquid Cell Setup with sample and copper wire, adhered with silver paint on AFM stage

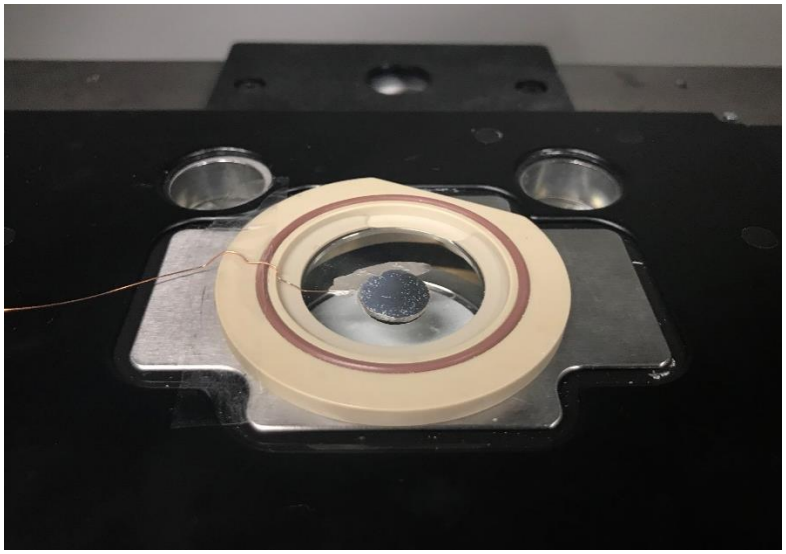

Figure A 9: Side View of Liquid Cell Setup with sample and copper wire, adhered with silver paint on AFM stage

Appendix B: Additional Tables

Property	Value
Yield Strength	41,000 psi
Thickness	0.080 inches
Hardness	120 Brinell
Temper	T3
Fabrication	Cold-Rolled
Specifications Met	ASTM B209
Heat Treatment	Hardened
Product No.	88835K71

Table B 1: Material Properties of Aluminum Alloy 2024-T3 [8]